# Author's Accepted Manuscript

UVA-induced Carbon-Centered Radicals in Lightly Pigmented Cells detected using ESR Spectroscopy

Nick Kassouf, Christopher W.M. Kay, Arsen Volkov, Shih-Chieh Chiang, Mark A. Birch-Machin, Sherif F. El-Khamisy, Rachel M. Haywood
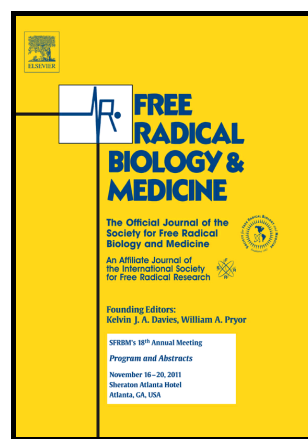
Cite this article as: Nick Kassouf, Christopher W.M. Kay, Arsen Volkov, Shih-Chieh Chiang, Mark A. Birch-Machin, Sherif F. El-Khamisy and Rachel M. Haywood, UVA-induced Carbon-Centered Radicals in Lightly Pigmented Cells detected using ESR Spectroscopy, *Free Radical Biology and Medicine*, https://doi.org/10.1016/j.freeradbiomed.2018.07.019

UVA-induced Carbon-Centered Radicals in Lightly Pigmented Cells detected using ESR Spectroscopy

Nick Kassouf[1], Christopher W. M. Kay[2,3], Arsen Volkov[1], Shih-Chieh Chiang[4], Mark A. Birch-Machin[5], Sherif F. El-Khamisy[4], Rachel M. Haywood[1*]

[1]RAFT Institute, Mount Vernon Hospital, Northwood, Middlesex, HA6 2RN, UK.

[2]Institute of Structural & Molecular Biology and London Centre for Nanotechnology, University College London, Gower Street, London WC1E 6BT, UK.

[3]Department of Chemistry, University of Saarland, 66123 Saarbrücken, Germany.

[4]Department of Molecular Biology and Biotechnology, University of Sheffield, Western Bank, Sheffield S10 2TN, UK.

[5]Dermatological Sciences, Institute of Cellular Medicine, The Medical School, Newcastle University, NE2 4HH, UK.

[*]Corresponding author. haywoodr@raft.ac.uk

Dedication: This paper is dedicated to the memory of our friend and colleague, Dr Katharina F. Pirker (1977-2015), who died as a result of malignant melanoma.

ABSTRACT

Ultraviolet-A and melanin are implicated in melanoma, but whether melanin *in vivo* screens or acts as a UVA photosensitiser is debated. Here, we investigate the effect of UVA-irradiation on non-pigmented, lightly and darkly pigmented melanocytes and melanoma cells using electron spin resonance (ESR) spectroscopy. Using the spin trap 5,5 Dimethyl-1-pyrroline *N*-oxide (DMPO), carbon adducts were detected in all cells. However, higher levels of carbon adducts were detected in lightly pigmented cells than in non-pigmented or darkly pigmented cells. Nevertheless, when melanin levels were artificially increased in lightly pigmented cells by incubation with L-Tyrosine, the levels of carbon adducts decreased significantly. Carbon adducts were also detected in UVA-irradiated melanin-free cell nuclei, DNA-melanin systems, and the nucleoside 2'-deoxyguanosine combined with melanin, whereas they were only weakly detected in irradiated synthetic melanin and not at all in irradiated 2'-deoxyguanosine. The similarity of these carbon adducts suggests they may be derived from nucleic acid– guanine – radicals. These observations suggest that melanin is not consistently a UVA screen against free-radical formation in pigmented cells, but may also act as a photosensitizer for the formation of nucleic acid radicals in addition to superoxide. The findings are important for our understanding of the mechanism of damage caused by the UVA component of sunlight in non-melanoma and melanoma cells, and hence the causes of skin cancer.

ABBREVIATIONS: DMPO, - 5,5 Dimethyl-1-pyrroline *N*-oxide; ESR, - Electron spin resonance spectroscopy; 8-oxodGuO, - 8-oxo-7,8-dihydro-2'-deoxyguanosine; UV, - Ultraviolet radiation ; UVA, - Ultraviolet-A radiation; UVB, - Ultraviolet-B radiation

Keywords: electron-spin-resonance spectroscopy**;** free radicals**;** Ultraviolet-A**;** melanocyte**;** melanoma.

INTRODUCTION

Epidemiological evidence, from studies of Australian migrants, links malignant melanoma in humans to intense sunlight exposure in childhood [1]. Experimental animal data demonstrates the induction of melanoma in neonatal transgenic mice exposed to a mixed ultraviolet-B/ultraviolet-A (UVB/UVA) light source [2, 3], and later using the same albino mouse model lacking melanin pigment the potency of ultraviolet-B (UVB) rather than ultraviolet-A (UVA) [4]. An earlier study using a pigmented fish model Xiphophorus, showed the efficacy of UVB, UVA and blue-visible light [5]. UVA and visible light are associated with lower photon energy than UVB, but are the major components of solar radiation penetrating the earth's atmosphere; and they penetrate skin to a greater extent [6]. Indeed, Agar *et al* [7] demonstrated more UVA than UVB finger print mutations in the basal layer in human skin squamous cell carcinoma and solar keratoses, consistent with the greater penetration of UVA.

The principal UVA chromophore in skin and skin cells is melanin [6] and although a physical screen, it can also act as a photosensitiser of reactive oxygen species [8, 9], and as a radical scavenger [10]. Red-haired Caucasians have the highest susceptibility to skin cancer, attributed to higher levels of phaeomelanin compared to eumelanin in this phenotype. Studies suggest that eumelanin and phaeomelanin are comparable in photoreactivity and photoformation of the superoxide radical anion ($O_2^{\bullet-}$) [11, 12]. The photoxicity of phaeomelanin may reflect instead its photodegradation during UVA irradiation [13]. In addition, our recent studies suggest that melanin may act as a photocatalyst of electron transfer from DNA to oxygen [14, 15]. Studies in which intact skin was irradiated generally suggest that melanin in the stratum corneum is photoprotective, and an effective screen against damage in the epidermis [15-18].

By contrast in isolated cells not protected by overlying melanin pigment in a stratum corneum, studies still conflict as to whether melanin is damaging or photoprotective. Pigmented melanocytes were shown to be protected against UVB-induced cyclobutane pyrimidine dimers (CPD) and (6-4) pyrimidone photoproducts (6-4PP) [19] but a later study showed little protection by melanocyte melanin against CPD induction in keratinocytes [20]. Melanin has been shown to protect against UVA-induced membrane damage [21]. In the absence of irradiation, melanin protects melanocytes and keratinocytes against H_2O_2-induced DNA strand breaks through its ability to bind Ca^{2+} [22]. Li and Hill found that melanin protected mouse melanoma cells from cell killing and mutation as measured by mutation induction at the Na+/K(+)-ATPase locus using ethyl methane sulfonate, and after irradiation

with monochromatic UVC and UVB. Significant protection against killing by polychromatic UVB + UVA was found, but not against mutation [23]. With respect to nuclear damage, 8-oxo-7,8-dihydro-2'-deoxyguanosine (8-oxodGuo) DNA damage is higher in UVA-irradiated melanoma cells stimulated to synthesise melanin [24]. DNA strand breaks are increased in melanocytes stimulated to increase melanin production, being highest in melanocytes from type VI individuals containing the highest levels of melanin pigment [25]. It is reported that TUNEL-positive cells (cells containing putative DNA double strand breaks), are 3-fold more frequent in black and yellow than in albino mice after UV irradiation [26]. It has recently been shown that chemiexcitation of melanin derivatives induces DNA cyclobutane pyrimidine dimer (CPD) photoproducts long after UV exposure [27].

Here we used ESR spectroscopy combined with spin-trapping, to address the role of melanin *in vivo* with respect to damage caused by UVA irradiation of normal cell lines, and melanoma cell lines with different levels of pigmentation. Furthermore, to obtain a deeper understanding of the source of the radicals observed, we also performed *in vitro* experiments on cell nuclei, and solutions containing various combinations of melanin, DNA and 2'-deoxyguanosine (dGuO).

MATERIALS AND METHODS

Cell Culture

Human melanoma cells, CHL-1 (amelanotic) and FM94 and SK23 (melanotic) were cultured in normal growth RPMI medium (Sigma) supplemented with 10% chelated FCS, 1% L-glutamine, 100 U/ml penicillin and 100 mg/ml streptomycin. Lightly- and darkly-pigmented human adult epidermal melanocytes (referred to as HEMa-LP and HEMa-DP, respectively) obtained from Invitrogen were cultured in 254 medium plus growth supplement (HMGS-2). All cells were incubated in 5% CO_2, 95% air atmosphere at 37 °C and the medium renewed every 2-3 days.

The relative melanin content of cells was estimated by two methods. (i) Biochemical Method: a known number of cells were incubated in 1 M NaOH for 2 h at 37 °C. The OD_{490} was then read and compared with that of a standard curve of synthetic melanin (Sigma). This approach gives relative rather than absolute cellular melanin concentrations because no correction for absorption by other cell components at 490 nm was made. (ii) ESR Method: The ESR spectrum of a known number of cells was measured in the dark. The observed melanin signal was fitted with two Lorentzian lines. Two are required to take into account the main signal and a weaker, low-field shoulder (possibly attributed to pheomelanin [28]) observed at higher *g*-value. The double integral of the fit was used as a measure of the relative amount of melanin.

Human skin fibroblasts (referred to as DF1098) were isolated from human skin obtained from consenting patients undergoing routine plastic surgery operations. The fat was removed and the skin cut into approximately $1mm^2$ pieces and placed on the surface of a T-25 culture flask. Skin pieces were immersed in 2-3 ml of normal growth medium (DMEM (Gibco)) supplemented with 10% chelated FCS, 1% L-glutamine, 100 U/ml penicillin and 100 mg/ml streptomycin. Flasks were observed at 3-4 day intervals for evidence of fibroblast migration, and tissue surrounded by migrating fibroblasts was removed, the media replaced and cells further cultured as for the melanoma cell lines except DMEM media was used instead of RPMI.

Preparation of Cells with the Spin Trap, DMPO

DMPO was purified before use by treatment with activated charcoal (1 g per 10 ml PBS). The DMPO solution could, at the high spin-trap concentration of 0.9 M DMPO, contain hydroxyl adducts as shown in Figure 1. Simulation gave hyperfine couplings (hfcs): a(H) =

1.47; a(N) = 1.49 mT. 30 minutes irradiation of this solution results in the increased presence of this adduct and slightly changed hfcs: a(H) = 1.48 mT; a(N) = 1.49 mT [29].

10^7 cells were incubated in 250 µl PBS containing DMPO (0.9 M) for 60 min, and then washed in 10 ml PBS to remove extracellular DMPO, and further re-suspended in 250 µl PBS prior to irradiation. This ensures that there is no extracellular DMPO outside the cell in the surrounding medium and all the DMPO is within the cell. Under these conditions, no hydroxyl adduct is observed.

Isolation of Mitochondria and Cell Nuclei

4×10^7 cells were harvested and washed in PBS then resuspended in 1 ml ice-cold mitoprep buffer (250 mM sucrose, 2 mM Hepes, 0.1 mM EGTA, pH: 7.4). Cells were transferred to a glass-Teflon homogeniser and disrupted with 20 strokes of a hand-drill motor driven Teflon plunger at 1000 rpm. Disrupted cells were then transferred to a fresh Eppendorf and centrifuged at 2200 rpm for 10 min at 4 °C using a benchtop centrifuge. The cell nuclei in the pellet containing containing nuclear DNA were stored at -80 °C. The pellet containing the mitochondrial fraction was transferred to a fresh Eppendorf on ice and centrifuged at 11000 rpm for 10 min at 4 °C. The supernatant in the centrifuged mitochondrial fraction was then removed and the mitochondrial pellet resuspended in 400 µl mitoprep buffer. Samples were then flash-frozen using liquid nitrogen and stored at -80 °C. We found that irradiation of mitochondria suspended in mitoprep buffer gave carbon and oxygen adducts, which were also detected in irradiated mitochondrial buffer medium alone For this reason, mitochondria were suspended in PBS for the experiments performed with mitochondria (data not shown).

DNA Extraction and Isolation

1×10^7 cells were harvested and resuspended in 200 µl resuspension buffer (75 mM NaCl, 25 mM EDTA, pH: 8). An equal volume of lysis buffer (10 mM Tris, 10 mM EDTA, 1% SDS, pH: 8) plus 400 µg/ml Proteinase K was added to cells, mixed gently and incubated at 50 °C for 3 h. Extraction of DNA was carried out using phenol/chloroform with centrifugation at 6500g and DNA was subsequently precipitated by adding absolute ethanol plus 3 M sodium acetate. The DNA pellet was finally air-dried, the dry weight determined, and the known dry weight (in the range 50 - 100 mg) resuspended in 0.4 ml sodium phosphate buffer (pH 7.4) and 50 µl 0.9 M DMPO for irradiation experiments. In experiments involving DNA with intrinsic melanin (Figure 5a) the 0.4 ml DNA was suspended in phosphate buffer and 50 µl

0.9 M DMPO was added prior to irradiation. DNA isolated from pigmented cells contains associated melanin unless electrophoresis is used to isolate it [30]. In experiments involving DNA without intrinsic melanin (Figure 5b,c) DNA solutions were prepared using salmon sperm DNA (Sigma) to 100 mg/ml in phosphate buffered saline (containing calcium and magnesium). 0.2 ml DNA solution was then mixed with 0.2 ml PBS, 50 μl 0.9 M DMPO in PBS, 1 mg tyrosine melanin (solid powder from Sigma synthesised from tyrosine and hydrogen peroxide) and the pH adjusted to be in the range 7 – 8 using 1M sodium hydroxide and pH indicator strips.

ESR Spectroscopy and Irradiation
ESR experiments were undertaken with a JEOL FA100 Spectrometer. Typical settings were 20 mW microwave power, 0.2 mT modulation, 2×10^3 signal amplitude, sweep time 5 s with repeated scanning (25 scans) and sweep width 10 mT. Inverted lines due to a reference manganese (typical of the JEOL spectrometer used to acquire this data) can be seen in spectra recorded using this spectrometer as the outer low- and high-field lines. For irradiation a 300 W Oriel Xenon lamp (ozone free) was used, and radiation > 260 nm passed through a water filter to remove infra-red radiation and then two optical glass filters (WG320 Schott filter 4-5 mm thickness, UQG Optics Ltd) to filter UVB/UVC. The filtered irradiation was passed through a liquid-light-guide transmitting 220 - 600 nm. An irradiance of 8.0 mW/cm^2 (UVA-visible light) was measured at the distance of the sample from the fibre-optic probe using an ILT1400-A Radiometer photometer equipped with a thermopile detector measuring radiation over the full spectral range. Using a ratio of 1:7 UVA to visible light from solar simulator spectral irradiance data (Oriel Instruments Light Sources Catalogue) it is estimated that the UVA irradiance at the position of the cells in the spectrometer was approximately 1 mW/cm^2 UVA. Cells were continuously irradiated in a flat cell *in situ* in the ESR spectrometer using a Xenon lamp system. The irradiation times were limited in some experiments due to the steady sedimentation of cells in the ESR cell which removes them from the irradiation beam. Using a hand held UVA meter (Tanita Ultraviolet monitor, Tanita UK) we measured a UK summer sunlight reading during June of 2.6 mW/cm^2 [14]. UVA radiation 320 - 400 nm is attenuated by 37% the incident intensity at a depth of 60 – 90 μm in human skin [6]. The skin epidermis and stratum corneum have a combined depth of 110 μm [6] therefore we estimate the incident intensity on the cells in the basal layer to be approximately 50% the incident intensity and of the order 1 mW/cm^2 for UK summer sunlight intensities. Cells were also exposed to a higher intensity irradiation, which was measured to be 19 mW/cm^2 (UVA-visible

light) at the position of the sample using the radiometer, and therefore 2.4 mW/cm^2 UVA using a ratio of 1:7 UVA to visible light. This is estimated to be equivalent to the intensity incident upon the basal layer in cells exposed to Mediterranean sunshine, since a peak UVA irradiance of sunlight was measured previously in Greece using a hand held light meter to be 5 mW/cm^2, and 6.7 mW/cm^2 in Australia in November with the same meter [14].

TDP1 Experiments

The recombinant TDP1 DNA repair enzyme was generated according to reference 31 and used at 16.83 µM concentration in PBS. Salmon sperm DNA (Sigma) was used as supplied and prepared to 100 mg / ml in phosphate buffer pH 7.4 and the pH adjusted to 7 using NaOH (1 M). 0.2 ml of DNA was mixed with either 0.2 ml of PBS (containing sodium and magnesium) as a control or 0.2 ml 16.8 µM TDP1 enzyme (1.2 mg /ml) and 50 µl DMPO added. Synthetic melanin (Sigma) (1-2 mg) was subsequently added and the pH readjusted to 7 prior to irradiating with UVA/visible light.

Melanin oxidation experiments

Soluble protein-melanin was synthesised using L-tyrosine (0.5g/100ml) and tyrosinase (1 – 5 mg) in pH 7 phosphate buffer with the inclusion of bovine serum albumin (BSA) (10 mg/ml) in the reaction mixture according to reference 9. DNA-melanin was similarly synthesised except salmon sperm DNA (Sigma) was used instead of BSA (data for Figure 7a). For the experiments in Figure 7b-c, synthetic tyrosine melanin (Sigma) was prepared at 0.5 mg/ml in phosphate buffer pH 7 by first solubilising 10 mg melanin in 100 µl 1M NaOH followed by dilution to 20 ml with buffer. The melanin solution was divided into two 10 ml solutions to which 200 mg of salmon sperm DNA (Sigma) was added to one and the other solution was left without DNA. The pH of both solutions was adjusted, using 1M NaOH, to be in the range 7-8 using pH indicator strips. Solutions were incubated at 37 ^{o}C and the UV/visible absorption spectra with time were recorded using a Nanodrop 2000 spectrometer over a period of 16-22 days.

A high DNA concentration was used since we estimated the nuclear concentration to be of the order of mg/ml according to the following calculation. If we assume 10 µg DNA is typically extracted per million cells, then the quantity of DNA per cell is 10 pg. The volume of a cell is calculated using the equation for the volume of a sphere, assuming that the size of an average cell is 10 µm diameter and thus 5 µm radius. The volume of a cell is calculated to be 5.24 × 10^{-16} m^3 which is 5.24 × 10^{-10} cm^3 (ml). An estimate for the weight of DNA per ml is

calculated from 1×10^{-11} divided by 5.24×10^{-10} which gives 0.019 g/ml (20 mg/ml). This is if the DNA is distributed evenly through the cell, which it is not. If the nucleus is taken to be 10% the volume of the cell, then the volume of the nucleus is 5.24×10^{-11} and the nuclear DNA concentration is estimated therefore to be 1×10^{-11} divided by 5.24×10^{-11} which is 200 mg/ml in a cell of 10 μm diameter. Since cells can vary in size up to 100 μm diameter then this estimate is an upper limit for a DNA concentration in the nucleus.

ESR Spectral Simulations

ESR spectral simulations were undertaken using MATLAB software (version R2016A Mathworks Inc.) and the EasySpin toolbox [32].

RESULTS

Highest level of carbon radical adduct formation is found in HEMa-LP cells containing intermediate levels of melanin

Figure 2a compares the ESR signals of a range of cell lines (melanoma and normal respectively) non-pigmented (CHL-1, DF1098); light-pigmented (FM94 and HEMa-LP); and dark-pigmented (SK23 and HEMa-DP) in the dark (left panel, red lines) and following 30 minutes of UVA irradiation (right panel, blue lines). In the dark, a broad transition comprising a main peak and a shoulder to the low field side was detected for all cells except CHL-1 and DF1098 cells that contain no melanin. This transition was fitted by two Lorentzian lines (left panel, black lines), and the double integral of the fit used to quantify the relative amounts of melanin radical present.

Following irradiation, a six-line spectrum of variable intensity was detected with all cells (right panel, blue lines). The spectra could all be fitted with hfcs: a(H) = 2.25 mT and a(N) = 1.60 mT, typical of a carbon adduct (right panel, black lines). Double integrals of the fits to the six line spectra (but excluding the melanin signal where present) were used to estimate the relative amount carbon adduct in each cell line.

Figures 2b and c show the relationship between the melanin radical signal from biochemical analysis and the weight of melanin from ESR versus the carbon adduct signal from ESR, respectively.

Inspection of the data provides reassurance that the ESR estimate of melanin radical in the dark (coloured red) and the biochemical measurement of melanin mass (coloured black) correlate well with each other. However, the striking result is that the intensity of the UVA-induced carbon adduct (coloured blue) increases initially with pigmentation, but subsequently decreases as the pigmentation increases further. Thus, the moderately pigmented HEMa-LP cells showed the greatest levels of carbon adducts, despite having an intermediate level of melanin.

Increasing the amount of melanin in HEMa-LP cells, reduces the amount of carbon radical adduct.

In the light of these results, we next investigated the effect of boosting the melanin concentration in lightly pigmented HEMa-LP cells on the formation of the UVA-induced carbon adducts, see Figure 3. After incubation with L-tyrosine (2 mM), a 66% mean increase in melanin per cell was determined compared to untreated cells using the biochemical method

(Figure 3c, magenta bars). Similarly, a comparison of ESR spectra of untreated and L-tyrosine treated cells in the dark shows an increase in the amount of melanin radical in the latter (Figure 3a and b, red lines). The spectra were fitted by two Lorentzian lines (Figure 3a and b, black lines), and the double integral of the fits used to obtain the relative amounts of melanin radical present (Figure 3c, red bars). With this approach, a 102% mean increase in melanin radical in L-tyrosine-treated cells compared to untreated cells was found. Following 30 min UVA-irradiation of cells, the ESR spectra contain carbon adducts superimposed on the melanin radical (blue lines). The spectra are similar to those presented in Figure 2a, and could be fitted with hfcs: a(H) = 2.24 mT and $\underline{a}$(N) = 1.60 mT (black lines). Again, the double integral of the fits (but excluding the melanin signal) was used to quantify the signal. This indicates that the amount of carbon adduct decreased to 44% in L-tyrosine treated cells compared to untreated cells (Figure 3c, blue bars).

Carbon radical adducts in (melanin-free) CHL-1 and DF1098 cells are associated with the nuclei.

To confirm that the adducts in melanin-free cells are associated with DNA damage, we irradiated nuclear fractions from CHL-1 and DF1098 cell lines. Figure 4 shows ESR spectra (coloured lines) and simulations (black lines) of isolated CHL-1 nuclei pre-incubated with the spin trap DMPO, in the dark and following irradiation with UVA. In the dark, a weak hydroxyl adduct is observed with a(H) = 1.54 mT and a(N) = 1.47 mT. Following UVA irradiation, as and found for DMPO alone (Figure 1), the intensity of this adduct increases by a factor 6, and additionally a carbon adduct, similar to that found in whole cells, with hfcs: a(H) = 2.22 mT and a(N) = 1.60 mT, is observed. Similar results were found for DF1098 cells. Irradiation of mitochondria from CHL-1 cells gave no observable DMPO adducts (data not shown).

Formation of carbon radical adducts in DNA/melanin systems at physiological pH.

Previously [14,15] we showed that when SK23 cell genomic DNA co-isolated with melanin was suspended in pH 4.5 phosphate buffer to high concentration (250 mg/ml) and UVA-irradiated with DMPO, carbon adducts were consistently detected often together with a broad resonance of a stable non-trapped radical.

Here, we studied DNA-melanin photoreactions under more physiological conditions. SK23 DNA with intrinsic melanin isolated from cells suspended in pH 7.4 phosphate buffer in the dark, showed the melanin spectrum composed of a main peak and a strong shoulder at

11

lower magnetic field (Figure 5a). Following UVA irradiation, in addition to the melanin signal, carbon adducts with hfcs: a(H) = 2.23 mT and a(N) = 1.60 mT, and hydroxyl adducts with hfcs: a(H) = 1.45 mT and a(N) = 1.51 mT were detected.

When Salmon sperm DNA was suspended with synthetic tyrosine melanin, a complex spectrum is observed (Figure 5b). Simulations allow identification of: a carbon adduct with hfcs: a(H) = 2.19 mT and a(N) = 1.57 mT; a hydroxyl adduct with hfcs: a(H) = a(N) = 1.49 mT; and a third species with hfcs: a(H) = 0.96 mT and a(N) = 1.46 mT which are similar to those reported for the $O_2^{\bullet-}$ adduct of DMPO [8]. Upon irradiation, a similar spectrum is observed, although the relative intensities of the components change slightly, with an increase in the intensity of the underlying melanin radical.

When the DNA 3'-end processing enzyme, TDP1, is added to this system, a similar spectrum is observed in the dark (Figure 5c). However, following UVA irradiation, rather than an increase in the amount of carbon adduct, a strongly enhanced signal from the peroxyl adduct (indicated by *) is observed.

Formation of carbon radical adducts in 2'-deoxyguanosine/melanin systems at physiological pH.

The DNA base, guanine, is considered the most likely target of oxidatively generated damage to DNA by $^1O_2$ and one-electron oxidants [33]. Hence, next we compared the effect of UVA irradiation on synthetic tyrosine melanin (Figure 6a), a mixture of synthetic tyrosine melanin and dGuo (Figure 6b) and dGuo (Figure 6c). In the presence of DMPO, tyrosine melanin and dGuO show only the hydroxyl adduct in the dark with hfcs: a(H) = 1.46 mT and a(N) = 1.49 mT. Following UVA irradiation, the intensity of this component increases, as expected from Figure 1, and in the tyrosine melanin sample a small amount of carbon adduct with hfcs: a(H) = 2.28 mT and a(N) = 1.63 mT is also detected.

The mixture of tyrosine melanin and dGuO also gives the hydroxyl adduct with hfcs: a(H) = 1.46 mT and a(N) = 1.49 mT, but additionally gives a peroxyl adduct with hfcs: a(H) = 1.02 mT and a(N) = 1.42 mT and a small amount of carbon adduct with hfcs: a(H) = 2.29 mT and a(N) = 1.64 mT even in the dark. Both the hydroxyl adduct and the carbon adduct increase following UVA irradiation.

Formation of carbon-adducts in melanin co-synthesised with DNA and evidence that melanin acts as a catalyst in DNA oxidation

We have demonstrated previously that melanin co-synthesised with the protein bovine serum albumin (BSA) is soluble and a model for melanoprotein in melanosomes *in vivo* [9]. We and others propose that melanin binds to DNA in the nucleus and acts as a photocatalyst in UVA photoxidation of DNA. Consistent with other reports, melanin is distinct in the nucleus of SK23 melanoma cells as shown by the photomicrograph in Figure 7a. To address the question of whether melanin bound to DNA transfers damage to DNA, we synthesised melanin from L-dopa and tyrosinase in the presence of bovine serum albumin protein (BSA) or salmon sperm DNA. The soluble protein-melanin and DNA-melanin were UVA-irradiated with DMPO. The ESR spectra in Figure 7a show the detection of a significant carbon-adduct (*) in melanin-DNA but not in melanin-protein.

To test the proposed mechanism that melanin can act as an electron transfer agent in the oxidation of DNA, we studied the autoxidation of melanin at $37^{o}C$ in the presence and absence of DNA using UV/visible spectroscopy (Figure 7b). Melanin alone in pH 7 phosphate buffer slowly oxidised over 22 days as indicated by the loss in absorbance at the longer visible wavelengths and increase in absorbance in the UV region < 300 nm, which is broadly consistent with previous observations [8]. Previously we established that melanin oxidation in alkali was associated with an initial increase in the melanin semiquinone radical (similar to that observed during UVA irradiation) followed by a slow decrease in intensity of this radical with time. It was concluded that autoxidation proceeded with the gradual conversion of melanin hydroquinone (reduced) groups to quinone (oxidised) moieties via the semiquinone radical. The ability to photosensitise $O_2^{\bullet-}$ production upon irradiation was not lost with oxidation which confirmed the oxidised quinone groups to be the UVA chromophore in the polymer [8]. Here, in the presence of DNA, melanin autoxidation was not observed and an increase in absorbance was observed > 300 immediately adjacent to the DNA absorbance which was here around 300 nm. The rate of increase was greater (approximately by a factor of 1.5 – 2) in the presence of melanin compared to its absence (data shown in Figure 7c and Figure 8a). The DNA-melanin showed a strong absorbance around 300 nm, as did DNA alone, at the high concentration used of 20 mg/ml at pH 7. We investigated the effect of pH and variation of concentration on the salmon sperm DNA. DNA not pH adjusted at 20 mg/ml (pH 3-4) was also associated with a narrow absorbance band around 300 nm although slightly shifted to shorter wavelengths compared to DNA adjusted to pH 7 (see Figure 8). When we

diluted the 20 mg/ml pH 7 sample to 400 µg/ml (in pH 7 phosphate buffer) the spectrum was comparable to that typically expected for DNA with an absorption maximum at 260 nm. A transition between these two types of spectrum was observed at 2 mg/ml DNA concentration.

DISCUSSION

Previous studies of UVA-irradiated non-pigmented skin cells have demonstrated formation of singlet oxygen ($^1O_2$), hydrogen peroxide (H_2O_2) and $O_2^{\bullet-}$ [34]. The spin trapping with DMPO of hydroxyl radicals in UV-irradiated keratinocytes has been reported [35]. In studies of UVA-irradiated melanosomes (which contain melanin bound by a lipid membrane) and DMPO, $O_2^{\bullet-}$ production was found to increase initially with melanin concentration at constant UVA fluence, and peak at 0.3 mg/ml melanin before subsequently declining above 0.3 mg/ml [11]. Although not a radical, $^1O_2$ forms a hydroxyl adduct upon trapping by DMPO [36]. In addition, the relatively unstable $O_2^{\bullet-}$ adduct can decay at physiological pH to a hydroxyl adduct. The hydroxyl adduct we detect *in vitro* (Figure 1) probably reflects, in part, contributions due to DMPO photolysis, and background levels of hydroxyl adducts already present in DMPO and in the presence of melanin, the trapping of $^1O_2$. In cells, hydroxyl adducts of DMPO are metabolically reduced to ESR silent species prior to irradiation, in contrast with no reduction *in vitro*. The lack $^1O_2$ of an intracellular hydroxyl adduct in intact cells (Figure 2) may reflect higher reactivity of and superoxide with macromolecules in the cell (or antioxidants such as superoxide dismutase) which are in high concentration compared to DMPO. In isolated nuclei, the DNA concentration is likely to be lower than that in nuclei of intact cells, and the presence and activity of antioxidants unknown. Photolysis of DMPO to a hydroxyl adduct in the cell is less likely in view of lower cell DMPO concentrations compared to the *in vitro* systems which were not washed, and where, as suggested above, a proportion of the hydroxyl adduct could reflect DMPO photolysis. An additional explanation, however, might be the difference in oxygen concentration in the cellular and non-cellular *in vitro* systems. The high density of actively metabolising cells in a small volume of buffer in the narrow-necked, and stoppered, ESR cell will likely become hypoxic, in contrast to non-metabolising nuclei and DNA-melanin. Thus, the formation of $O_2^{\bullet-}$, $^1O_2$ and therefore hydroxyl adducts would be expected to be reduced in cells compared to the *in vitro* systems.

We have shown that UVA-irradiation of non-pigmented and pigmented skin cells preloaded with DMPO consistently gives an ESR detectable carbon adduct

14

(Figure 2). This adduct is formed intra-cellularly since it is detected after removal of extracellular DMPO by washing. The carbon adduct in our experimental system is highest in cells with low levels of melanin compared to non-pigmented or highly pigmented cells and decreases in light pigmented cells stimulated to increase in melanin synthesis (Figure 3). Similar findings were reported by O Chiarelli-Neto *et al* in studies of melanocytes exposed to visible light, where phototoxic effects were greater in intermediate pigmented cells compared to non-pigmented or more darkly pigmented cells [37]. Wenczl *et al* showed that in melanocytes exposed to UVA, DNA damage in the form of strand breaks increased with melanin content and was highest at high pigment concentrations found in type VI melanocytes [25]. This may reflect different experimental conditions: in the latter study single cell layers were used by contrast with multiple cell layers in the ESR cell used in our experiments, which can contribute screening effects. It is noteworthy that if these experiments were repeated with the more penetrating visible light, different results might be obtained at the higher melanin concentrations. It is also possible that the carbon adducts formed in pigmented cells are underestimated in our experiments, due to their greater rates of cell sedimentation compared to non-pigmented cells, when held upright in the ESR flat cell. Slow cell sedimentation during the irradiation and ESR measurement results in their removal from the irradiation beam and imposes a limit on the time of irradiation.

We suggest that the carbon adduct detected here in cells (Figures 2,3) is a trapped nucleic acid radical, since a comparable carbon adduct is detected in UVA-irradiated isolated cell nuclei (Figure 4) and in DNA-melanin systems (Figure 5). We previously detected a carbon adduct in human DNA isolated from amelanotic (lacking melanin) and pigmented melanoma cells (containing intrinsic melanin after extraction) at low pH (4.5). This pH was studied previously due to the greater solubility of DNA in acid and stability of the protonated $O_2^{\bullet-}$ (hydroperoxyl) radical, which can be detected at low pH, as we demonstrated in UVA-irradiated dopa melanin and melanosomes isolated from hair [9,11]. At a DNA concentration of 100 mg/ml in pH 4.5 buffer, carbon adducts and the hydroperoxyl adduct of DMPO were both detected [14,15]. In those studies, both the carbon and $O_2^{\bullet-}$ adducts were abolished by superoxide dismutase. The signal intensity of the carbon adducts was lower in amelanotic compared to melanotic DNA. In addition, when we irradiated commercially available salmon sperm DNA with tyrosine melanin in pH 4.5 buffer, we also detected carbon adducts. The only other biological macromolecule which formed carbon adducts on UVA-irradiation was soybean phospholipid [15]: the phospholipid carbon adducts were more anisotropic with

slightly greater β-H splitting than those detected in irradiated cells or DNA-melanin. Whilst we suggest that the carbon adducts detected in cells correspond to nucleic acid carbon adducts, we cannot exclude the possibility that they include lipid radical contributions either all or in part. In irradiated model phospholipid systems alkoxyl adducts are distinct after irradiation, and believed to result from re-arrangement of peroxyl adducts trapped subsequent to addition of oxygen to conjugated dienyl radicals [15]. However, alkoxyl adducts could not be detected in cells post-irradiation.

When present, melanin is the principal chromophore for UVA and it is believed to form an oxidising triplet state upon photoexcitation [38]. In earlier work, we established that irradiation of solubilised dopa melanin [8,9] and sepia melanin (from squid ink) gave the hydroperoxyl adduct of DMPO together with low levels of the hydroxyl adduct at pH 4.5. Low levels of a carbon adduct could be detected when sepia melanin was initially concentrated by dissolving in sodium hydroxide but were no longer detected when the concentrated solution was diluted further in pH 4.5 buffer and irradiated. These low levels of carbon radicals are believed to be due to the increase in melanin autoxidation as the pH increases [8]. The photoreactions of UVA-irradiated melanin are summarised in reference 9, and are proposed to comprise electron transfer from melanin (in the absence of an external electron donor) to molecular oxygen with the formation of $O_2^{\bullet-}$ and the resultant oxidation of melanin, see Figure 9. At low melanin concentrations photosensitised formation of $O_2^{\bullet-}$ predominates and $O_2^{\bullet-}$ is trapped by DMPO. At high concentrations melanin reacts with $O_2^{\bullet-}$ (acting as a radical scavenger) and levels of DMPO-trapped $O_2^{\bullet-}$ decrease. There is now evidence that melanin also photosensitises $^1O_2$ formation, which at 450 nm is very low (quantum yield $\sim 10^{-4}$) but which strongly increases in the UV region [39].

For melanin to act as a photocatalyst in DNA oxidation it would have to be in close proximity to DNA. Melanin binds to the minor groove in DNA promoting strand breaks, with eumelanin being more harmful than phaeomelanin in this study [40]. We, and others [24,25], proposed that this could occur by melanin leaking from UVA-damaged melanosomes (UVA-induced membrane holes from lipid peroxidation) into the surrounding cytoplasm and nucleus. In addition, during nuclear DNA replication, DNA lacking protection by histone proteins and a nuclear membrane is exposed to the cytoplasm and can interact with melanin and metal-ions, which can strongly bind DNA [41]. In view of the short irradiation times used, it is possible that the nucleic acid carbon adducts we detect correspond initially to DNA/RNA damage in the cell cytoplasm, with nuclear contributions at longer times. The only

organelle where we identified carbon adducts was the cell nucleus, but we did not examine the cytoplasmic component. Predominant cytoplasmic location of UVA-radical damage was found by Swalwell *et al* who found mitochondrial DNA damage to decrease with melanin pigmentation [42]. This is in marked contrast to the effect on nuclear DNA damage in cells stimulated to increase melanin synthesis [24,25]. A possible explanation for these different effects is that melanin cannot penetrate the mitochondrial membrane but can penetrate the nuclear membrane whose charge is less tightly regulated.

When melanin is bound or associated with DNA, one possible reaction is that UVA-photosensitised singlet oxygen reacts with DNA to produce 8-oxodGuo DNA damage according to a non-radical Diels Alder [2 + 4] cycloaddition mechanism [33]. To account for the detection of radical intermediates we propose that a second electron transfer reaction may take place in which dGuo, the most readily oxidised DNA base, acts as an electron donor to the excited triplet of melanin, which acts as a photocatalyst for the oxidation of DNA and the reduction of oxygen (Figure 9). Evidence for melanin acting as a photocatalyst is provided by Rozanowska et al [43] who demonstrated that in the presence of the reductant ascorbate, melanin photosensitises electron transfer, superoxide formation and the oxidation of ascorbate. In addition, our experiments with dGuO (Figure 6) and to study melanin autoxidation in the presence and absence of DNA (Figures 7-8) support this, with melanin increasing the rate of change of the absorbance > 300 nm by a factor of 1.5 – 2 compared to DNA alone. This is consistent with previous findings of the relative formation of carbon-centered radicals in UVA-irradiated human SK23 DNA containing intrinsic melanin, compared to non-pigmented human DNA [14]. Interestingly, the absorption spectrum of DNA-melanin and DNA alone, was associated with a narrow absorption band around 300 nm and not 260 nm which is typically associated with DNA, which reflected the high concentration of DNA used in our study and not the pH (Figure 8). The effect of concentration here, where some precipitation may be present (although not visibly obvious), might reflect a transition between the B form of DNA (which is favoured in conditions of high water content) and the A form (the biological form which is favoured in conditions of low water). We have chosen to work with these high concentrations of DNA, because estimates of the DNA concentration in the cell nucleus were consistent with mg/ml concentrations. It is noteworthy that UVB (290 – 320 nm) is proposed to be directly absorbed by DNA with the formation of CPD [33]. This would be consistent with DNA being at high concentration in the cell nucleus and associated with an absorption band around 300 nm,

which is in the UVB region. The DNA absorption band at 260 nm measured at low concentrations is in the UVC region of the spectrum and not UVB.

Our work here on DNA-melanin suspended in a physiological pH 7.4 buffer also demonstrates the formation of UVA-induced carbon adducts (Figure 5); however, the signals due to the carbon adduct are weaker at pH 7 (Figure 5b) than at low pH suggesting a lower stability of carbon radicals (or the adduct) at physiological pH or reaction with available oxygen to form peroxyl radicals**.** The carbon adduct may have small contributions due to UVA-oxidised melanin, Figure 6a. The detection of carbon adducts in the nucleoside dGuO UVA-irradiated in the presence of tyrosine melanin, but not present in dGuO alone and greater than those in tyrosine melanin alone, supports the hypothesis that guanine could be an electron donor in this system (Figure 6). In view of the relatively mobile (isotropic) nature of the carbon adducts, the radicals appear to have some mobility either in the free nucleoside or when on intact DNA (or DNA fragments).

The only spin-trapped DNA radical (generated by $^\bullet$OH) characterised so far is the 6-aminyl radical derived from adenine in DNA exposed to Cu(II) and hydrogen peroxide, although in that study, a nitrogen-centred species was detected [44]. More recently, however, guanine neutral radicals G(-H)$\bullet$ were formed from electrochemical oxidation of guanine and trapped by the nitrone spin trap PBN at the nitrogen (N3) position in the free nucleoside, although different tautomeric forms have been proposed for the oxidising radical including those with the unpaired electron located at oxygen, C8, C5 and N3 [45]. In intact DNA, G(-H)$\bullet$ was trapped through carbon and not nitrogen. The authors of this study write "Indeed the disappearance of the second nitrogen coupling points out addition of PBN to a carbon and confirms that the radical trapping may take place before hydration. In this case, the (PBN) addition would take place through C8". G(-H)$\bullet$ does not react with oxygen but can react with $O_2^{\bullet-}$ [46]. The authors of this study write " Our study showed that the combination of G(-H)$\bullet$ and $O_2^{\bullet-}$ radicals in both single- and double- stranded DNA results in the formation of imidazolone lesions as the major products. Cadet and co-workers proposed that the Iz lesions can be formed via the 5-OOH-G(-H) hydroperoxide intermediates. Here formation of 5-HOO-G(-H) can occur by the addition of $O_2^{\bullet-}$ to the C-5 position of the G(-H)$\bullet$ radical followed by rapid protonation of the peroxide anion". That the main addition reaction takes place at C5 is indirectly shown by the formation of 2,2,4-triamino-5-(2H) oxazolone [47] but it would be of interest to establish this further in future studies using [13C] or [15N]-labelled dGuo. Both nitrones PBN and DMPO are known to trap carbon, oxygen and sulphur radicals,

but differ in that the beta hydrogen splitting of PBN adducts is relatively invariant, by contrast with DMPO adducts which are readily distinguished by the beta hydrogen splitting. Thus similar reactions might be expected of PBN and DMPO.

Deprotonation from first formed guanine radical cations (G•$^+$) is predominant upon 1-electron oxidation of dGuO, and the formation of G(-H)• competes with hydration of G•$^+$ and formation of the DNA oxidation product 8-oxo-7,8-dihydro-2'-deoxyguanosine (8-oxodGuo). G•$^+$ (which is stabilised in native DNA) is usually hydrated to form 8-hydroxy-7,8-dihydroxguanyl, that upon molecular oxygen-mediated one-electron oxidation, is converted into 8-oxo 7,8-dihydroguan-7-yl radical. Competitive one-electron reduction has been found to give rise to 2,6-diamino-4-hydroxy-5-formamidopyrimidine (FapyGua) [48,49]. Intermediates of the hydration reactions of G•$^+$ may also be able to react with spin traps in aerated aqueous solutions.

The effect of the oxidatively generated DNA damage repair enzyme TDP1 to increase the observed amount of a peroxyl adduct *in vitro*, suggests that TDP1 and DMPO compete for a DNA radical which would otherwise react with a peroxyl radical. If TDP1 reacts more rapidly with a nucleic acid - guanine radical than DMPO, then O_2•$^-$ would be expected to react instead with DMPO. The effect of TDP1 in a cell system, was higher levels of carbon adducts but without the liberation of a peroxyl radical, in TDP1-deficient compared to wild type cells [31]. This, again, would be consistent with the relative hypoxia of cells compared to DNA-melanin *in vitro*.

To conclude, we detect carbon radicals in UVA-irradiated cells in an ESR experimental system, using high cell densities in the ESR flat cell which are likely to be hypoxic. Carbon radicals are known to react rapidly with oxygen and would not be expected to be readily detected under normoxic conditions (as we observe at pH 7 *in vitro*). In addition, hypoxic conditions would favour conversion of G•$^+$ to G(-H)•, which does not react with oxygen but which can be spin trapped by PBN and presumably DMPO. Our findings show that unscreened melanocytes containing low levels of melanin pigment (under equivalent experimental conditions) are more susceptible to UVA-induced carbon radical damage than non-pigmented cells. Whilst studies suggest melanin in the stratum corneum screens against epidermal cell damage within intact skin, we show it does not shield unscreened isolated cells containing low pigmentation against UVA-induced carbon radical formation, when they are exposed to irradiation intensities comparable to those which would be incident upon cells in the skin basal layer exposed to Mediterranean sunshine. In practical terms the presence of an

overlying protective melanin layer in the stratum corneum will reduce the UVA intensity incident on sensitive cells in the basal layer and reduce cellular free radical damage. In skin not adequately protected by an overlying layer of melanin pigment in the stratum corneum (white Caucasian untanned skin or skin exposed to high UVA intensities), basal cells, particularly those with low levels of melanin pigment will be the most vulnerable to UVA damage. Our study raises further questions as to the identity, location and mechanisms of formation of the carbon radicals and their link with biological damage. The findings, however, may open up important avenues in investigating the causation of skin damage and possibly melanoma by UVA.

AUTHOR CONTRIBUTIONS

ESR experiments were performed by RH and NK with support from AV. ESR simulations and figures were made by CK. Data analysis was performed by RH, NK and CK. TDP1 was prepared by S-C C under the supervision of S E-K. The paper was written by RH with CK supported by NK. The study was conceived by RH and MB-M and supervised by RH.

REFERENCES

[1]   Khlat, M.; Vail, A.; Parkin, M.; Green, A. Mortality from melanoma in migrants to Australia: variation by age at arrival and duration of stay. *American journal of epidemiology* **135**, 1103-1113; 1992.

[2]   Noonan, F. P.; Dudek, J.; Merlino, G.; De Fabo, E.C. Animal models of melanoma: an HGF/SF transgenic mouse model may facilitate experimental access to UV initiating events. *Pigment cell research / sponsored by the European Society for Pigment Cell Research and the International Pigment Cell Society* **16**, 16-25; 2003.

[3]   Noonan, F. P.; Recio, J.A.; Takayama, H.; Duray, P.; Anver, M.R.; Rush, W.L.; De Fabo, E.C.; Merlino, G. Neonatal sunburn and melanoma in mice. *Nature* **413**, 271-272; 2001.

[4]   De Fabo, E. C.; Noonan, F.P.; Fears, T.; Merlino, G. Ultraviolet B but not ultraviolet A radiation initiates melanoma. *Cancer research* **64**, 6372-6376; 2004.

[5]   Setlow, R. B.; Grist, E.; Thompson, K.; Woodhead, A.D. Wavelengths effective in induction of malignant melanoma. *Proceedings of the National Academy of Sciences of the United States of America* **90**, 6666-6670; 1993.

[6]   Anderson, R. R.; Parrish, J.A. The optics of human skin. *The Journal of investigative dermatology* **77**, 13-19; 1981.

[7]   Agar, N. S.; Halliday,G.M.; Barnetson, R.S.; Ananthaswamy, H.M.; Wheeler, M.; Jones, A.M. The basal layer in human squamous tumors harbors more UVA than UVB

fingerprint mutations: a role for UVA in human skin carcinogenesis. *Proceedings of the National Academy of Sciences of the United States of America* **101**, 4954-4959; 2004.

[8]   Haywood, R. M., Lee,M.; Linge, C.;. Synthetic melanin is a model for soluble natural eumelanin in UVA-photosensitised superoxide production. *Journal of photochemistry and photobiology. B, Biology* **82**, 224-235; 2006.

[9]   Haywood, R. M.; Linge, C. An experimental and theoretical model for solar UVA-irradiation of soluble eumelanin: towards modelling UVA-photoreactions in the melanosome? *Journal of photochemistry and photobiology. B, Biology* **76**, 19-32; 2004.

[10]   Bustamante, J.; Bredeston, L.; Malanga, G.; Mordoh, J. Role of melanin as a scavenger of active oxygen species. *Pigment cell research / sponsored by the European Society for Pigment Cell Research and the International Pigment Cell Society* **6**, 348-353; 1993.

[11]   Haywood, R. M.; Lee, M.; Andrady, C. Comparable photoreactivity of hair melanosomes, eu- and pheomelanins at low concentrations: low melanin a risk factor for UVA damage and melanoma? *Photochemistry and photobiology* **84**, 572-581; 2008.

[12]   Sarna, T.; Menon, L.A.; Sealy, R.C. Photoinduced oxygen consumption in melanin systems--II. Action spectra and quantum yields for pheomelanins. *Photochemistry and photobiology* **39**, 805-809; 1984.

[13]   Chedekel, M. R.; Smith, S.K.; Post, P.W.; Pokora, A.; Vessell, D.L. Photodestruction of pheomelanin: role of oxygen. *Proceedings of the National Academy of Sciences of the United States of America* **75**, 5395-5399; 1978.

[14]   Haywood, R.; Andrady, C.; Kassouf, N.; Sheppard, N. Intensity-dependent direct solar radiation- and UVA-induced radical damage to human skin and DNA, lipids and proteins. *Photochemistry and photobiology* **87**, 117-130; 2011.

[15]   Haywood, R.; Rogge F.; Lee, M. Protein, lipid, and DNA radicals to measure skin UVA damage and modulation by melanin. *Free radical biology & medicine* **44**, 990-1000; 2008.

[16]   Brenner, M.; Hearing, V.J. The protective role of melanin against UV damage in human skin. *Photochemistry and photobiology* **84**, 539-549; 2008.

[17]   Herrling, T.; Jung. K.; Fuchs, J. The role of melanin as protector against free radicals in skin and its role as free radical indicator in hair. *Spectrochimica acta. Part A, Molecular and biomolecular spectroscopy* **69**, 1429-1435; 2008.

[18]   Yamaguchi, Y.; Takahashi, K.; Zmudzka, B.Z.; Kornhauser, A.; Miller, S.A.; Tadokoro, T.; Berens, W.; Beer, J.Z.; Hearing, V.J. Human skin responses to UV radiation:

pigment in the upper epidermis protects against DNA damage in the lower epidermis and facilitates apoptosis. *FASEB journal : official publication of the Federation of American Societies for Experimental Biology* **20**, 1486-1488; 2006.

[19]   Smit, N. P., Vink, A.A.; Kolb, R.M.; Steenwinkel, M.J.; van den Berg, P.T.; van Nieuwpoort, F.; Roza, L.; Pavel, S. Melanin offers protection against induction of cyclobutane pyrimidine dimers and 6-4 photoproducts by UVB in cultured human melanocytes. *Photochemistry and photobiology* **74**, 424-430; 2001.

[20]   Mouret,S., Forestier, A., Douki, T. The specificity of UVA-induced DNA damage in human melanocytes. *Photochem Photobiol Sci.* 11, 155-62; 2012

[21]   Kvam, E.; Dahle, J. Pigmented melanocytes are protected against ultraviolet-A-induced membrane damage. *The Journal of investigative dermatology* **121,** 564-569; 2003.

[22]   Hoogduijn, M. J.; Cemeli, E.; Ross, K.; Anderson, D.; Thody, A.J.; Wood, J.M. Melanin protects melanocytes and keratinocytes against H_2O_2-induced DNA strand breaks through its ability to bind Ca^{2+}. *Experimental cell research* **294**, 60-67; 2004.

[23]   Li, W.; Hill, H.Z. Induced melanin reduces mutations and cell killing in mouse melanoma. *Photochemistry and photobiology* **65**, 480-485; 1997.

[24]   Kvam, E.; Tyrrell, R.M. The role of melanin in the induction of oxidative DNA base damage by ultraviolet A irradiation of DNA or melanoma cells. *The Journal of investigative dermatology* **113**, 209-213; 1999.

[25]   Wenczl, E.; Van der Schans, G.P.; Roza, L.; Kolb, R.M.; Timmerman, A.J.; Smit, N.P.; Pavel, S.; Schothorst, A.A. (Pheo)melanin photosensitizes UVA-induced DNA damage in cultured human melanocytes. *The Journal of investigative dermatology* **111**, 678-682; 1998.

[26]   Takeuchi, S.; Zhang, W.; Wakamatsu, K.; Ito, S.; Hearing, V.; Kraemer, K.H.; Brash, D.E. Melanin acts as a potent UVB photosensitizer to cause an atypical mode of cell death in murine skin. *Proceedings of the National Academy of Sciences of the United States of America* **101**, 15076-15081; 2004.

[27]   Premi S,; Wallisch, S.; Mano, C.M.; Weiner A.B.; Bacchiocchi. A.; Wakamatsu, K.; Bechara, E.J.; Halaban, R.; Douki, T., Brash, D.E. Chemiexcitation of melanin derivatives induces DNA photoproducts long after UV exposure. *Science.* **347**, 842-7; 2015. doi: 10.1126/science.1256022

[28]. Sealy, R. C.; Hyde, J.S.; Felix, C.C.; Menon, I.A.; Prota, G.; Swartz, H.M.; Persad, S.; Haberman, H.F. Novel free radicals in synthetic and natural pheomelanins: distinction

between dopa melanins and cysteinyldopa melanins by ESR spectroscopy. *Proceedings of the National Academy of Sciences of the United States of America* **79**, 2885-2889; 1982.

[29]   Chignell, C. F., Motten, A.G.; Sik, R.H.; Parker, C.E.; Reszka, K. A spin trapping study of the photochemistry of 5, 5 dimethyl-1-pyrroline *n*-oxide (DMPO). *Photochemistry and photobiology* **59**, 5-11; 1994.

[30]   Price, K.; Linge, C. The pesence of melanin in genomic DNA isolated from pigmented cell lines interferes with successful polymerase chain reaction : a solution . *Melanoma Research* **9**, 5-9; 1999.

[31]   Chiang, SC.; Meagher, M.; Kassouf, N.; Hafezparast, M.; McKinnon, P.J.; Haywood, R.; El-Khamisy, S.F. Mitochondrial protein-linked DNA breaks perturb mitochondrial gene transcription and trigger free radical-induced DNA damage. Sci Adv. 2017 Apr 28;3(4):e1602506. doi: 10.1126/sciadv.1602506. eCollection 2017 Apr

[32] Stoll, S.; Schweiger, A. EasySpin, a comprehensive software package for spectral simulation and analysis in EPR *J. Magn. Reson.* **178**, 42-55; 2006.

[33]   Cadet. J.; Douki, T.; Ravanat J-L. Oxidatively generated damage to cellular DNA by UVB and UVA radiation. *Photochem Photobiol,* **91**, 140-155; 2015.

[34]   Vile, G. F.; Tyrrell, R.M. UVA radiation-induced oxidative damage to lipids and proteins in vitro and in human skin fibroblasts is dependent on iron and singlet oxygen. *Free radical biology & medicine* **18**, 721-730; 1995.

[35]   Taira, J., K.; Mimura, T.; Yoneya, A.; Hagi, A. Murakami and K. Makino. Hydroxyl radical formation by UV-irradiated epidermal cells. *Journal of biochemistry* **111**, 693-695; 1992.

[36]   Nishizawa, C., Takeshita, K.; Ueda, J.; Mizuno, M.; Suzuki, K.T.; Ozawa, T. Hydroxyl radical generation caused by the reaction of singlet oxygen with a spin trap, DMPO, increases significantly in the presence of biological reductants. *Free radical research* **38**, 385-392; 2004.

[37]   O Chiarelli-Neto Melanin photosensitisation and the effect of visible light on epithelial cells PLoS One, 9 (11),e113266; 2014.

[38] Wang, A.; Marino, A.R.; Gasyna, E.M.; Sarna, T.; J.R. Norris, Jr . Investigation of Photoexcited States in Porcine Eumelanin through Their Transient Radical Products *J. Phys. Chem. B*. **113***,* 10480–10482; 2009.

[39]   Szewczyk. G.; Zadlo, A.; Sarna, M.; Ito, S.; Wakamatsu, K.; Sarna, T. Aerobic photoreactivity of synthetic eumelanins and pheomelanins: generation of singlet oxygen and

superoxide anion. *Pigment Cell Melanoma Res.* **29**, 669-678; 2016. doi: 10.1111/pcmr.12514. Epub 2016 Sep 23.

[40]   Suzukawa, A. A.; Vieira, A.;Winnischofer, S.M.; Scalfo, A.C.; Di Mascio, P.; Ferreira, A.M.; J.L. Ravanat.; Martins Dde, L.; Rocha, M.E.; Martinez, G.R. Novel properties of melanins include promotion of DNA strand breaks, impairment of repair, and reduced ability to damage DNA after quenching of singlet oxygen. *Free radical biology & medicine* **52**, 1945-1953; 2012.

[41]   Geng, J.; Yuan, P.; Shao, C.; Yu, S.B.; Zhou, B.; Zhou, P.; Chen, X.D. Bacterial melanin interacts with double-stranded DNA with high affinity and may inhibit cell metabolism in vivo. *Archives of microbiology* **192**, 321-329; 2010.

[42]   Swalwell, H.; Latimer, J.; Haywood, R.M.; Birch-Machin, M.A. Investigating the role of melanin in UVA/UVB- and hydrogen peroxide-induced cellular and mitochondrial ROS production and mitochondrial DNA damage in human melanoma cells. *Free radical biology & medicine* **52**, 626-634; 2012.

[43]   Rozanowska, M.; Bober, A.; Burke, J.M.; Sarna, T. The role of retinal pigment epithelium melanin in photoinduced oxidation of ascorbate. *Photochemistry and photobiology* **65**, 472-479; 1997.

[44]   Bhattacharjee, S.; Jiang, J.; Sinha, B.K.; Mason, R.P. Detection and imaging of the free radical DNA in cells-site-specific radical formation induced by Fenton chemistry and its repair in cellular DNA as seen by electron spin resonance, immuno-spin trapping and confocal microscopy. *Nucleic Acids Res.* **40**, 5477-86; 2012.

[45]   Ribaut, C.; Bordeau, G.; Perio, P.; Reybier, K.; Sartor, V.; Reynes, O.; Fabre, PL.; Chouini-Lalanne, N. EPR spectroelectrochemical investigation of guanine radical formation and environment effects. *J Phys Chem B.* **118**: 2360-5; 2014.

[46]   Misiaszek, R.; Crean, C.; Joffe, A.; Geacintov, N.E.; Shafirovich, V. Oxidative DNA damage associated with combination of guanine and superoxide radicals and repair mechanisms via radical trapping. *Journal of Biological Chemistry* **279**, 32106-32115.

[47]   Jean Cadet, Maurice Berger, Garry W. Buchko, Prakash C. Joshi, Sebastien Raoul, Jean-LucRavanat. 2,2-Diamino-4-[(3,5-di-O-acetyl-2-deoxy-.beta.-D-erythro-pentofuranosyl)amino]-5-(2H)-oxazolone: a Novel and Predominant Radical Oxidation Product of 3',5'-Di-O-acetyl-2'-deoxyguanosine .*J Am Chem Soc* 116, 7403–7404, 1994.

[48] Cadet,J., Davies, K.J.A, Medeiros, M.H, Di Mascio, P., Wagner, J.R. Formation and repair of oxidatively generated damage in cellular DNA. *Free Radic Biol Med.* **107**:13-34; 2017.

[49]   Rokhlenko, Y., Cadet, J., Nicholas E., Geacintov, N.E, Shafirovich, V. Mechanistic Aspects of Hydration of Guanine Radical Cations in DNA *J. Am. Chem. Soc.*, **136**, 5956–5962, 2014.

Fig 1: ESR spectra of 0.9 M DMPO in PBS non-irradiated and during 30 min UVA-irradiation.

Fig 2: ESR spectra (a) control non-irradiated (dark) and obtained during 30 min UVA-irradiation of cultured human skin cells non-pigmented (CHL-1 and DF1098) and melanin-pigmented human melanocytes (HeMa-LP, HEMa-DP) and melanoma cells (SK23 and FM94) containing DMPO. (b-c) Plots of the integrated spectra of the carbon adduct in the above spectra versus the melanin content (pg /cell) in all cells determined using biochemical and ESR methods respectively. For each cell line (except melanoma cell lines where n = 2) the carbon adduct measurement is a mean of 3 independent experiments where cell sedimentation in the flat cell was observed to be minimal.

Fig 3: ESR spectra obtained before (dark) and during 30 min UVA irradiation of a) untreated and b) L-tyrosine-treated (2 mM for 7 days in culture) (representative of three separate spectra) HEMa-LP cells containing DMPO. (c) Bar charts showing relative melanin content by biochemical method (purple) and ESR method (red) and the carbon adduct (blue) in both control and L-tyrosine treated HEMa-LP spectra.

Fig 4: ESR spectra prior to irradiation (dark) and during 30 min UVA irradiation of cell nuclei isolated from CHL-1 cells and DMPO.

Fig 5: Dark (non-irradiated) and UVA-irradiated ESR spectra of (a) Genomic DNA extracted from SK23 cells (up to 100 mg dry weight suspended in 0.4 ml pH 7.4 buffer) and 50 μl 0.9 M DMPO (final concentration 180 mM). (b) Salmon sperm DNA (20 mg/ml), tyrosine melanin (ca. 0.2-0.4 mg/ml) and DMPO (180 mM) pH adjusted to 7 immediately prior to irradiation; (c) as for b) but including TDP1 DNA damage repair enzyme (6.7 μM).

Fig 6: Dark (non-irradiated) and UVA-irradiated ESR spectra of a) Tyrosine melanin (ca. 0.2 – 0.4 mg/ml) suspended in pH 7.4 phosphate buffer; b) 2'-deoxyguanosine (dGuO) (0.4 ml saturated solution in pH 7.4 phosphate buffer) and tyrosine melanin (0.5 - 2 mg) and 50 μl 0.9 M DMPO. c) 2'-deoxyguanosine (0.4 ml saturated solution in pH 7.4 buffer) and 50 μl 0.9 M DMPO.

Fig 7: A) Photomicrograph at high magnification of adherent pigmented SK23 melanoma cells in culture and ESR spectra of UVA-irradiated L-dopa melanin synthesised from L-dopa

and tyrosinase in the presence of salmon sperm DNA or bovine serum albumin (10 mg/ml) and the spin trap DMPO. B) UV/visible absorption spectra of synthetic tyrosine melanin (0.5 mg/ml) without (pink line) and with (blue line) salmon sperm DNA (20 mg/ml) at pH 7 and allowed to autoxidise at $37^{o}C$ for 528 hr (minus DNA- yellow line and plus DNA- grey line). C) UV/visible absorption spectra of salmon sperm DNA (20 mg/ml) and synthetic melanin (pH 7) during 16 days autoxidation.

Fig 8: a) UV/visible absorption spectra of salmon sperm DNA alone (20 mg/ml and pH 7) during 16 days autoxidation and b) comparison of UV/visible absorption spectra at pH 7 (blue line) at pH 3-4 (brown line) and diluted (in pH 7 buffer) to 10 mg/ml (lilac dotted line), 2 mg/ml (yellow dotted line), 800 ug/ml (blue dotted line), and 400 ug/ml (green line).

Fig 9: Putative reaction scheme for the production of carbon centred radicals and superoxide by melanin photosensitisation. Following UVA excitation, melanin forms a long-lived excited triplet state. This can undergo electron transfer (ET) with molecular oxygen form $O_2^{\bullet-}$, in which case it functions as a reductant. Alternatively, it can undergo ET with the DNA base, guanine to form a guanine radical cation $G\bullet^{+}$ (which in the scheme is denoted $G(H)\bullet^{+}$) in which case it functions as an oxidant. Note that $G\bullet^{+}$ rapidly deprotonates to form guanine neutral radicals $G(-H)\bullet$ following formation (in the scheme denoted $G\bullet$). In combination, these two reactions suggest that melanin acts as a photocatalyst to reduce molecular oxygen and oxidise guanine.

Figure 1

Figure 2

Figure 3

Figure 4

Figure 5

Figure 6

Figure 7

**ACCEPTED MANUSCRIPT**

a

b

c

Figure 8

ACCEPTED MANUSCRIPT

a

b
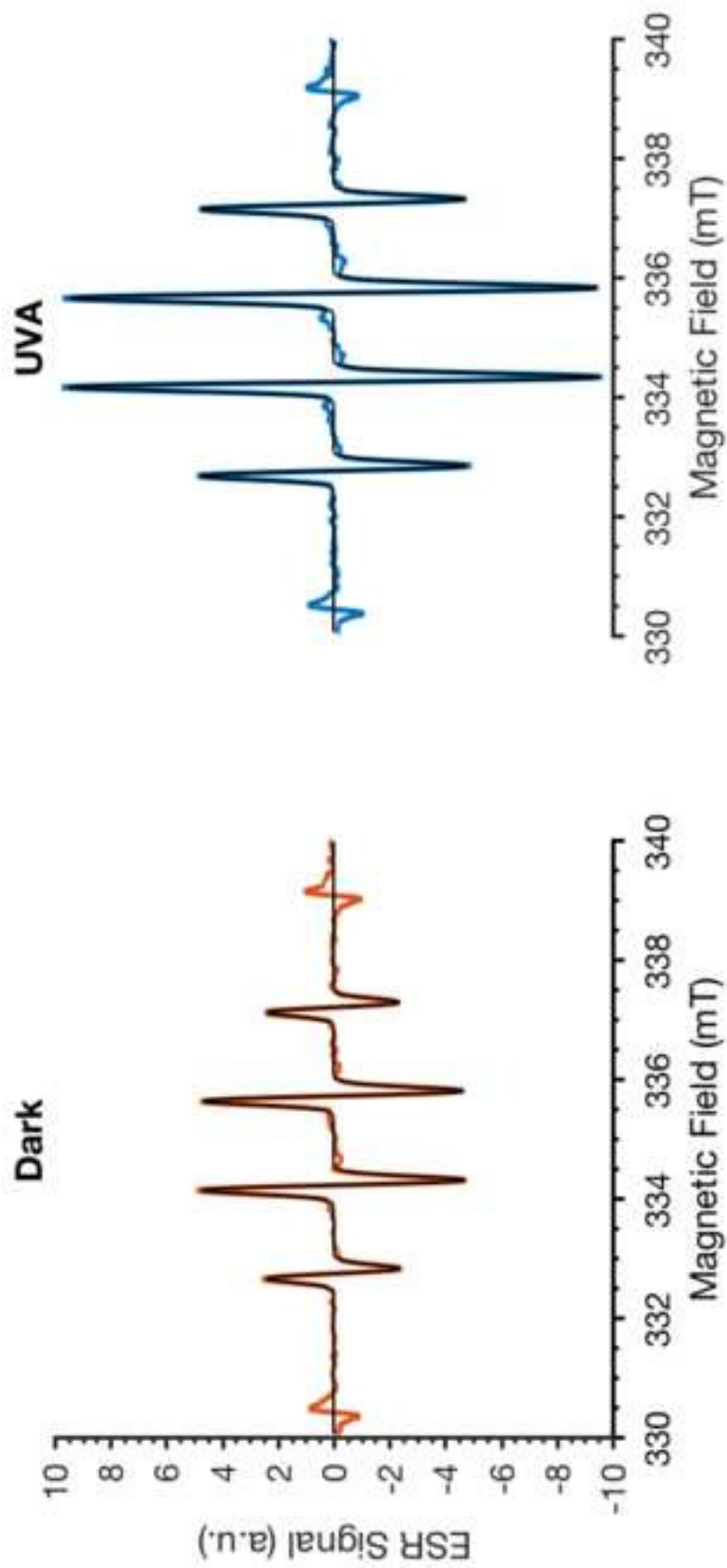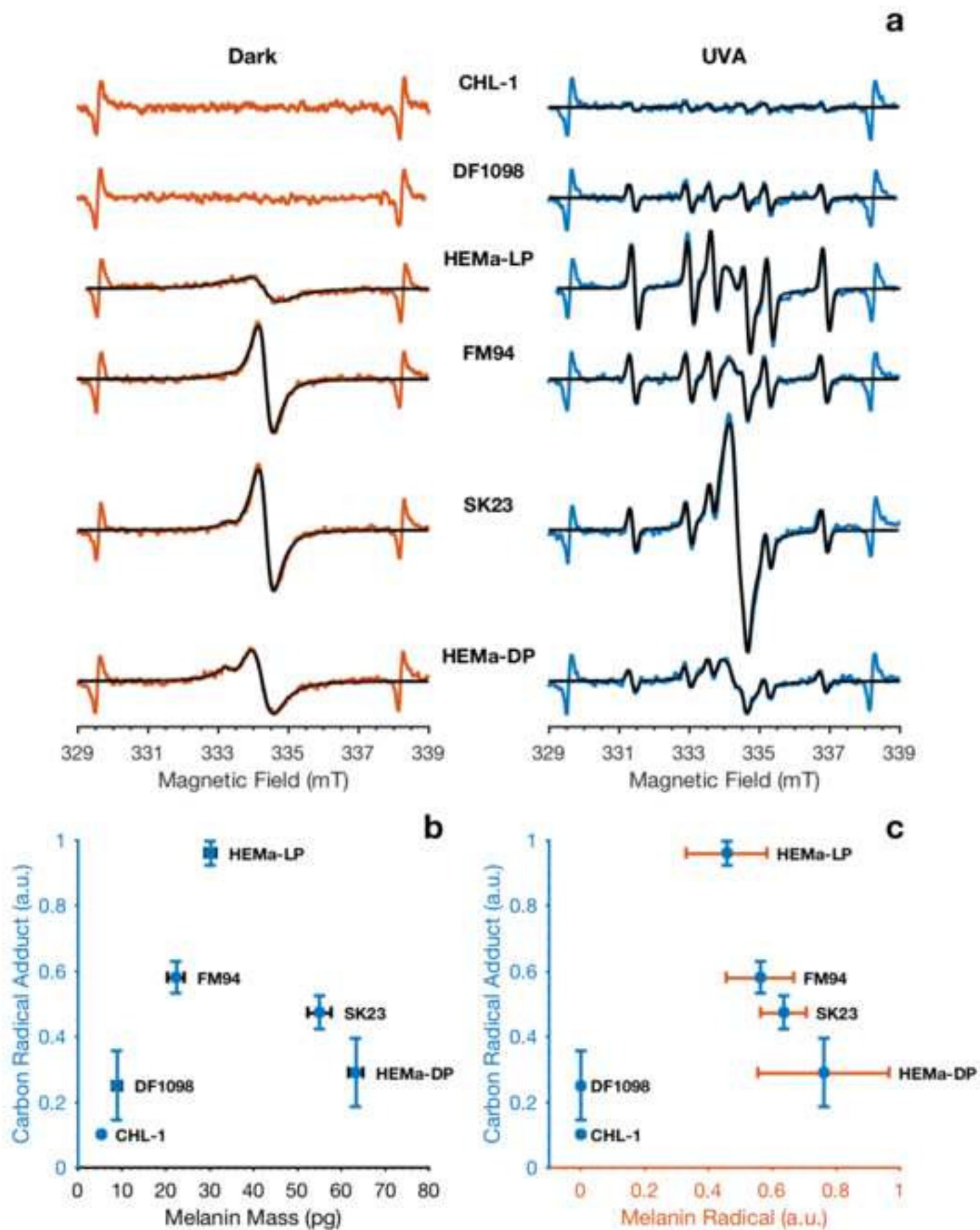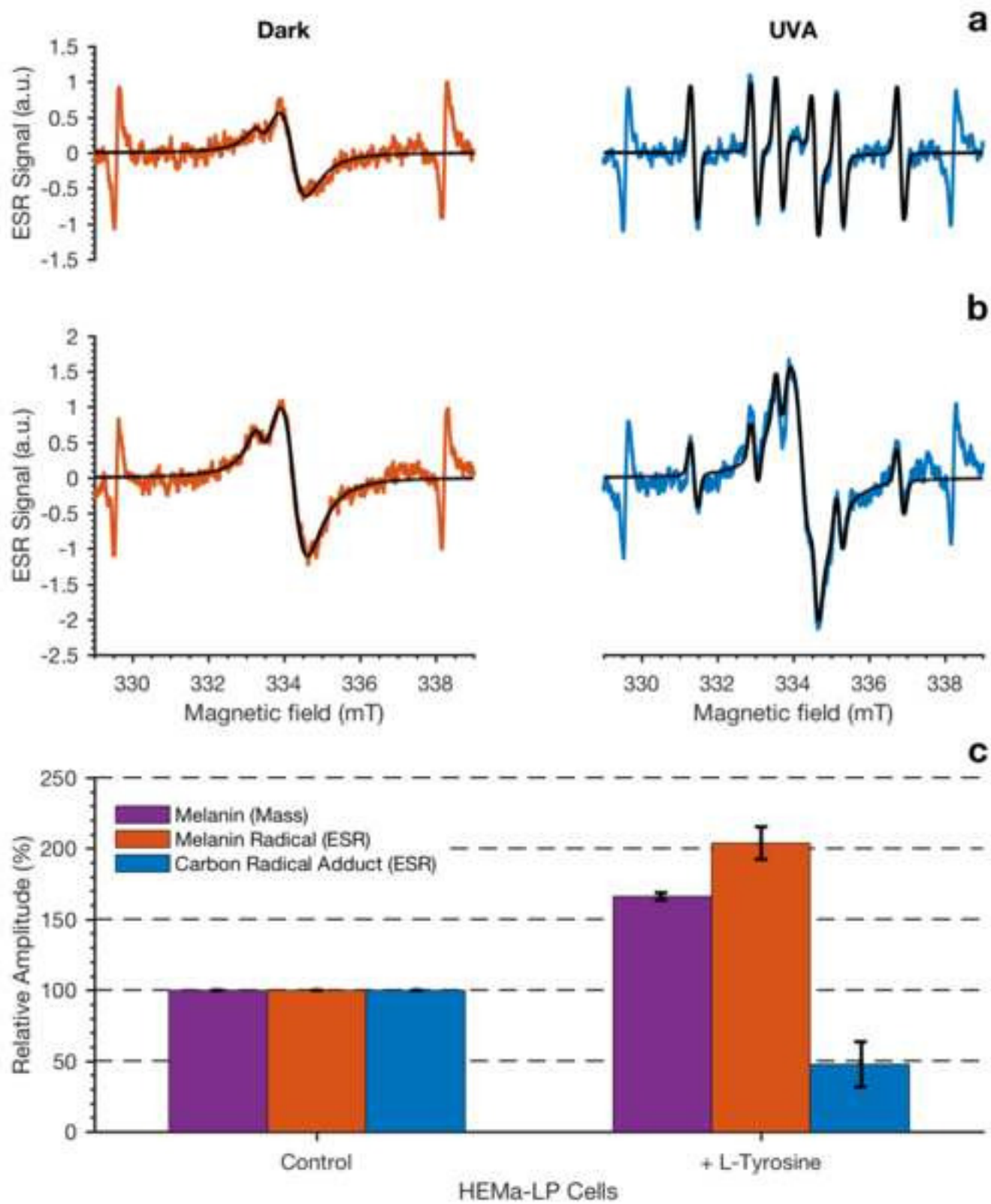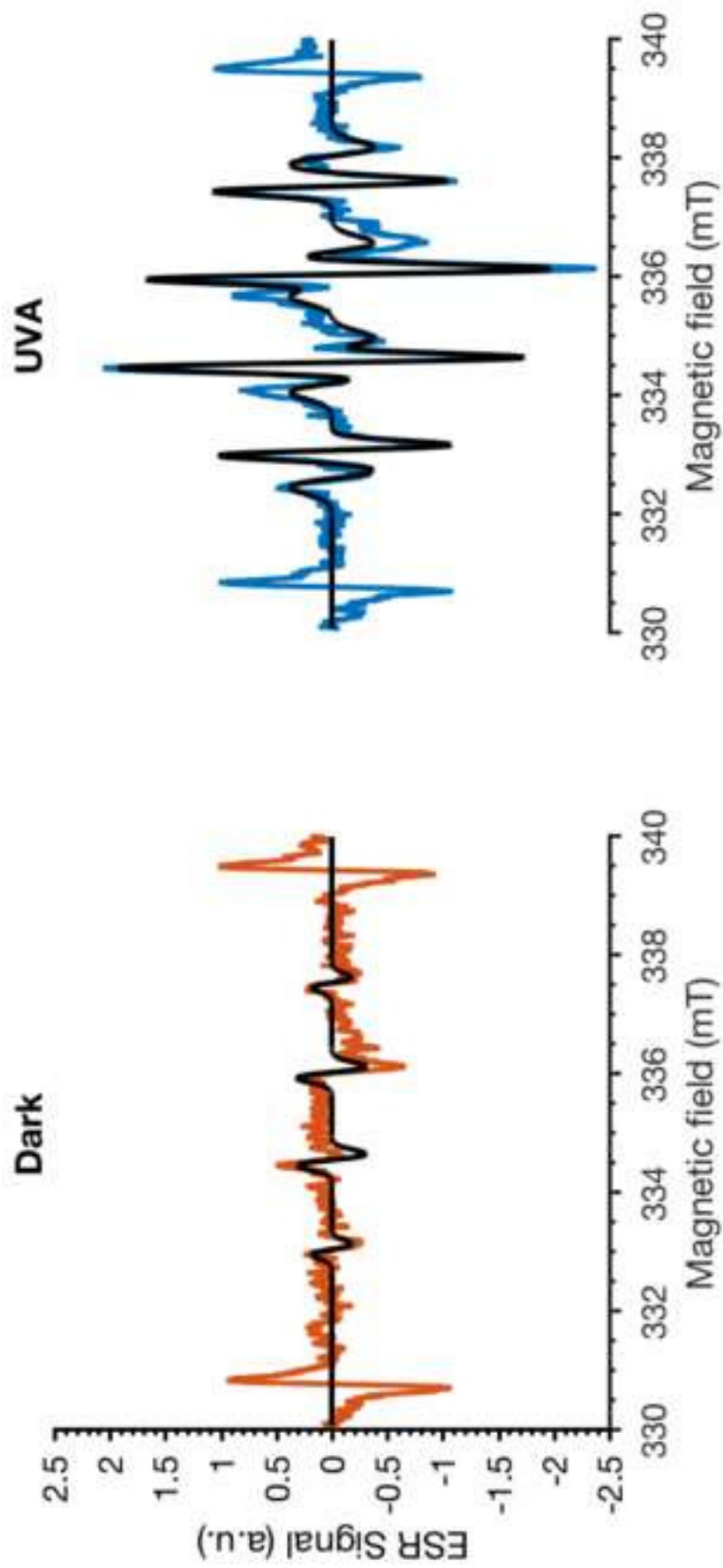
Figure 9
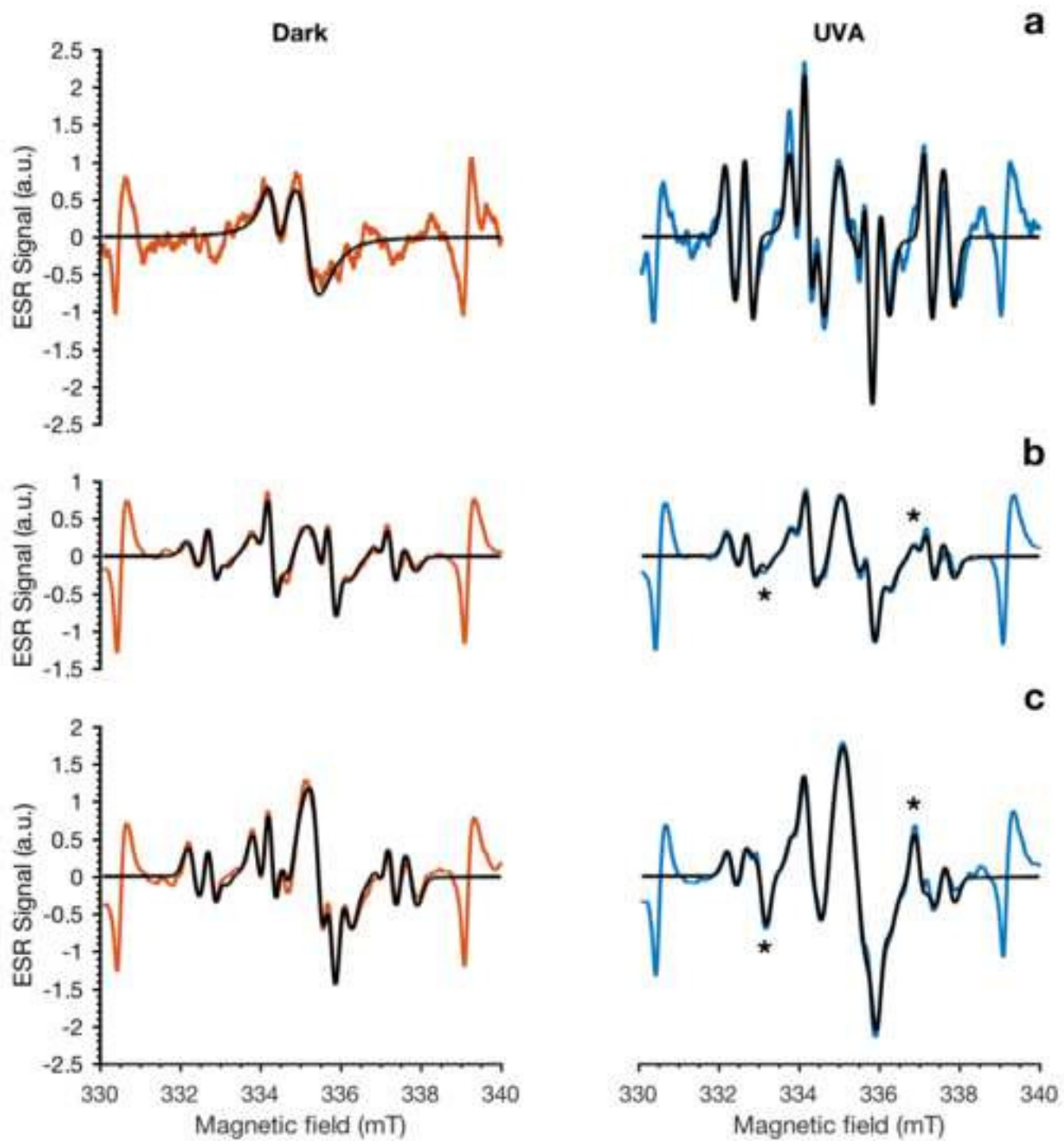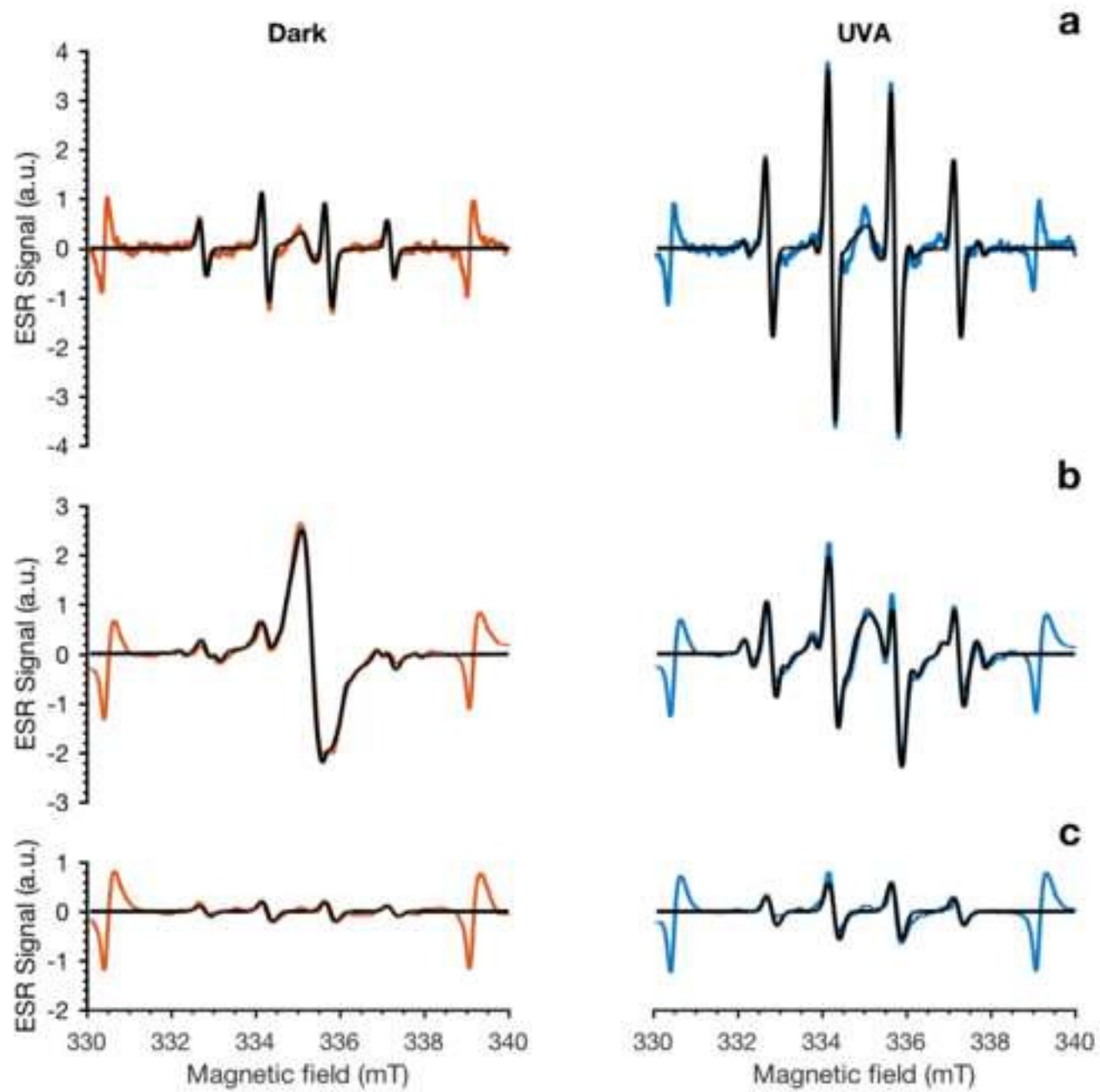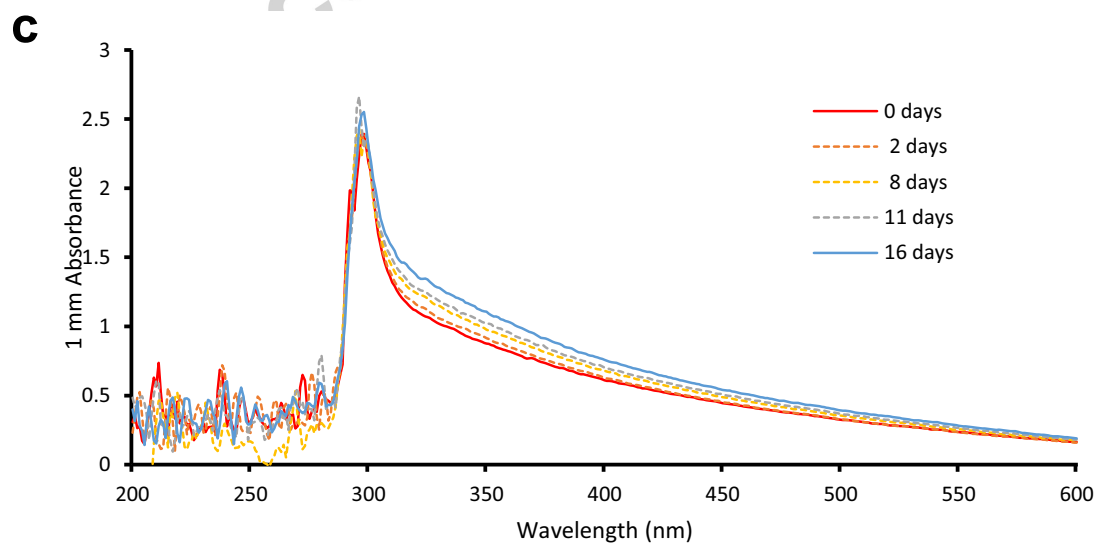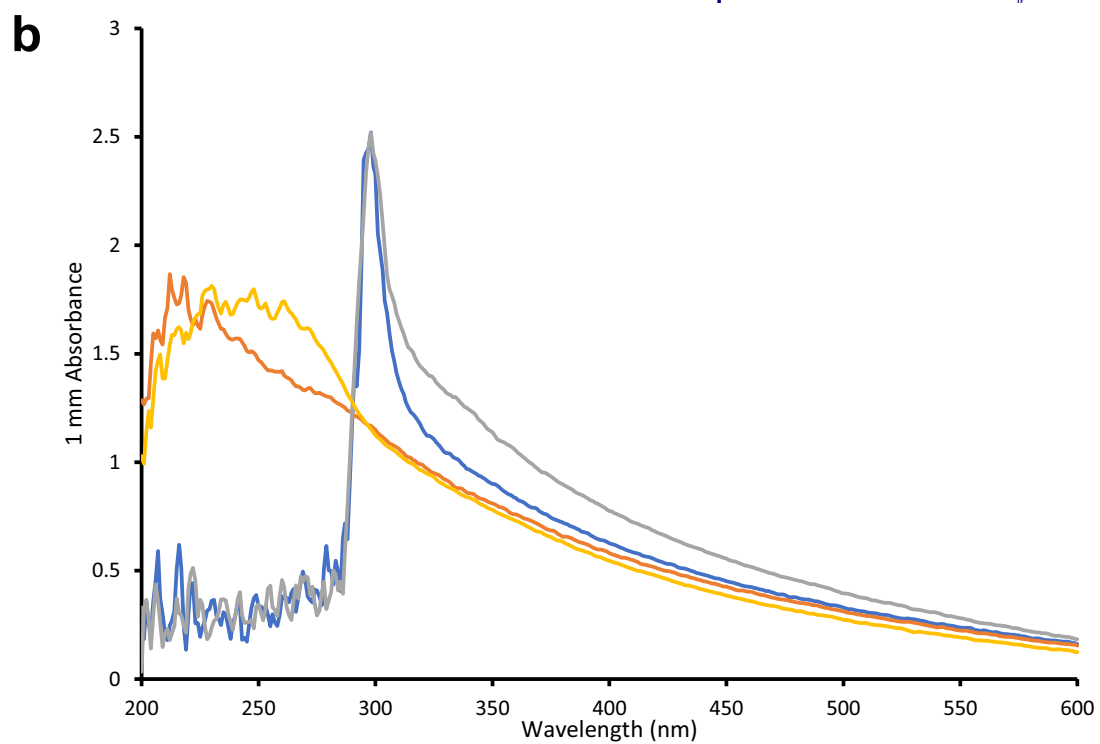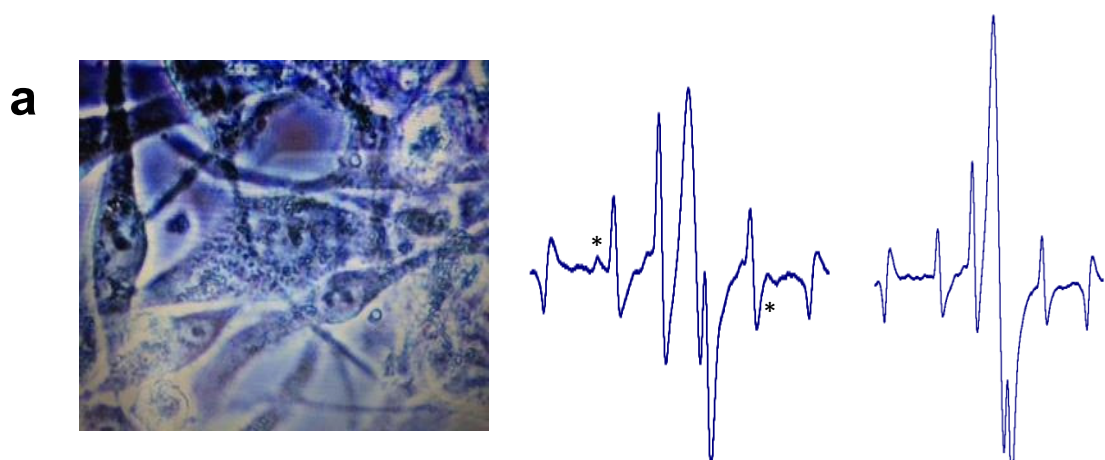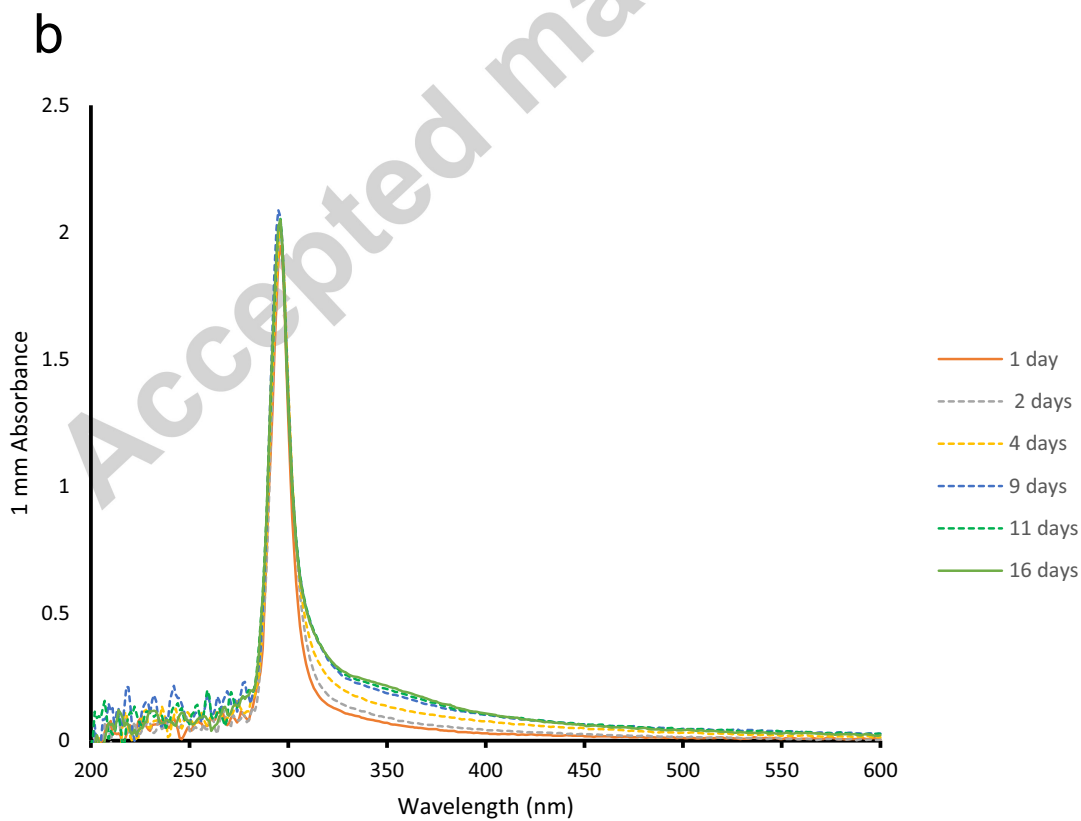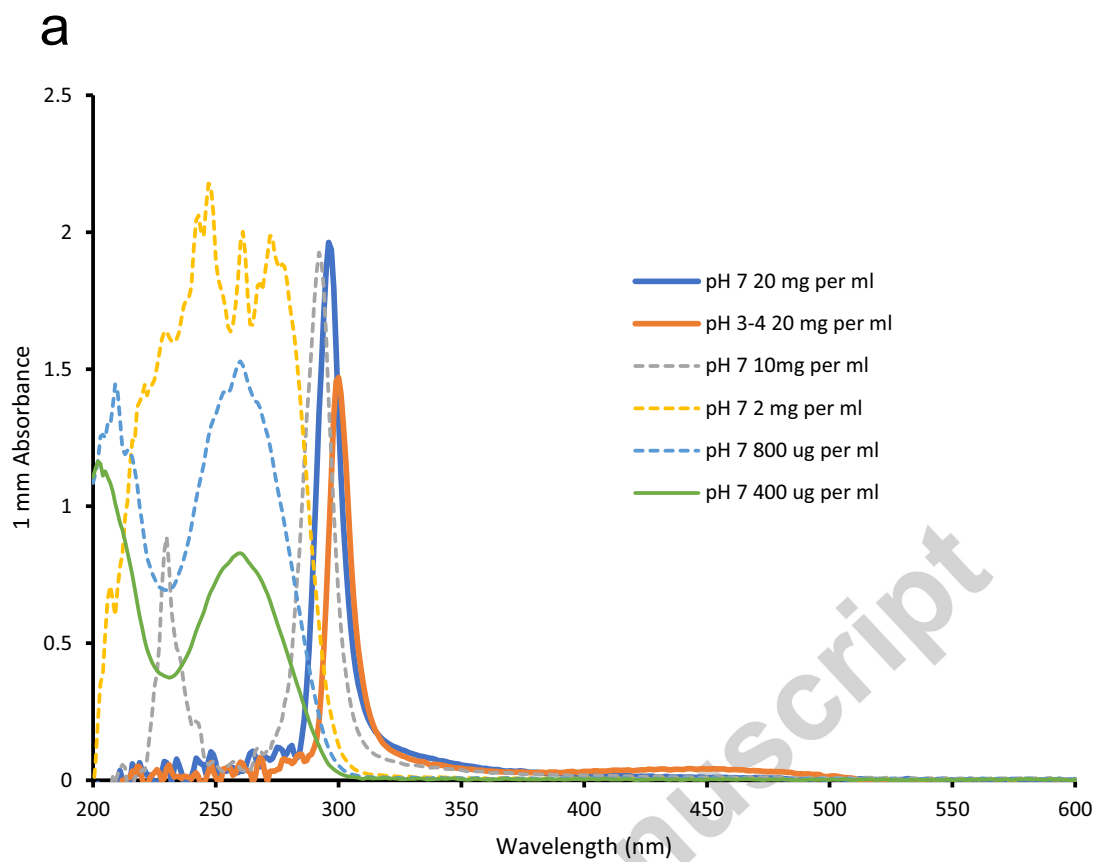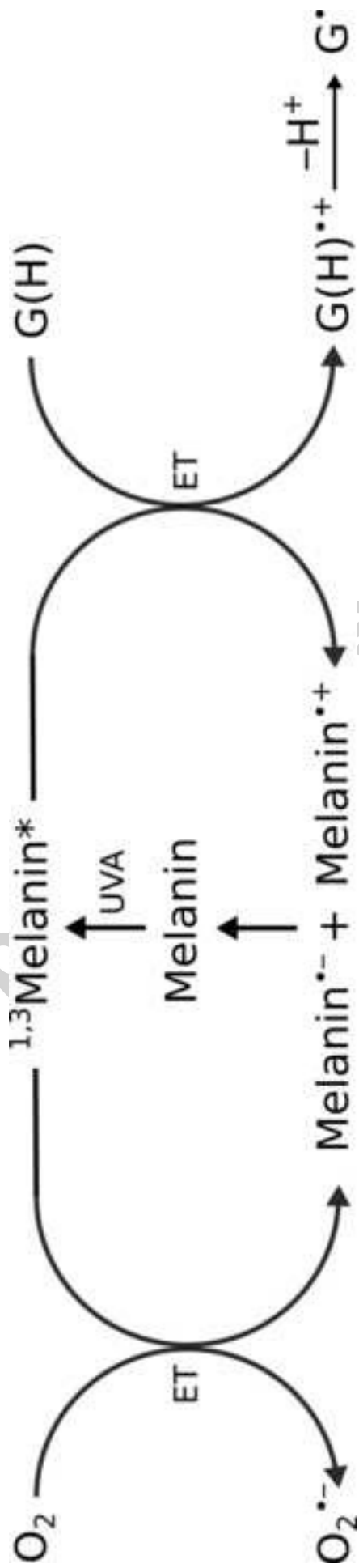
Non-pigmented and melanin-pigmented skin cells

UVA

melanosomes

Cell nucleus

DNA -melanin

Melanin Mass (pg)

Carbon Radical Adduct (a.u.)

HEMa-LP

FM94

DF1098

CHL-1

SK23

HEMa-DP
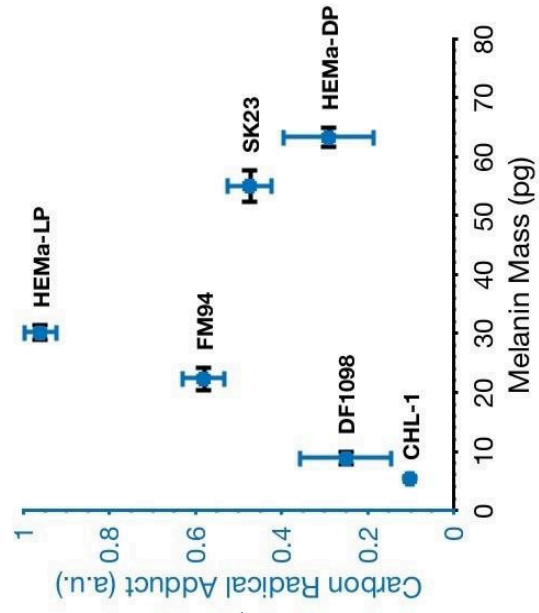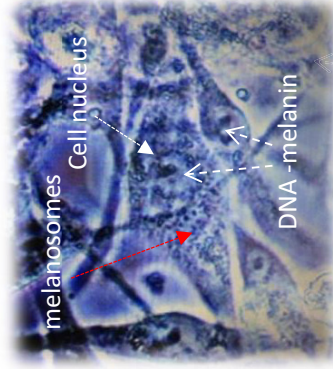
Highlights

- Carbon radicals are detected in UVA-irradiated cells
- Carbon radicals higher in light melanin-pigmented cells than cells without pigment
- Increase in melanin in light pigmented cells decreases radical levels
- Carbon radicals detected in cell nuclei, DNA-melanin and 2'-deoxyguanosine
- Carbon radicals proposed nucleic acid - guanine - radicals